Published OnlineFirst August 24, 2012; DOI: 10.1158/1078-0432.CCR-12-0861

Cancer Therapy: Preclinical

Clinical Cancer Research

Arylsulfonamide KCN1 Inhibits *In Vivo* Glioma Growth and Interferes with HIF Signaling by Disrupting HIF-1α Interaction with Cofactors p300/CBP

Shaoman Yin[1], Stefan Kaluz[1,5], Narra S. Devi[1], Adnan A. Jabbar[2], Rita G. de Noronha[6], Jiyoung Mun[3], Zhaobin Zhang[1], Purushotham R. Boreddy[8], Wei Wang[8], Zhibo Wang[4], Thomas Abbruscato[8], Zhengjia Chen[4], Jeffrey J. Olson[1,5], Ruiwen Zhang[8], Mark M. Goodman[2,3,5], K.C. Nicolaou[6,7], and Erwin G. Van Meir[1,2,5]

Abstract

Purpose: The hypoxia-inducible factor-1 (HIF-1) plays a critical role in tumor adaptation to hypoxia, and its elevated expression correlates with poor prognosis and treatment failure in patients with cancer. In this study, we determined whether 3,4-dimethoxy-*N*-[(2,2-dimethyl-*2H*-chromen-6-yl)methyl]-*N*-phenylbenzenesulfonamide, KCN1, the lead inhibitor in a novel class of arylsulfonamide inhibitors of the HIF-1 pathway, had antitumorigenic properties *in vivo* and further defined its mechanism of action.

Experimental Design: We studied the inhibitory effect of systemic KCN1 delivery on the growth of human brain tumors in mice. To define mechanisms of KCN1 anti-HIF activities, we examined its influence on the assembly of a functional HIF-1α/HIF-1β/p300 transcription complex.

Results: KCN1 specifically inhibited HIF reporter gene activity in several glioma cell lines at the nanomolar level. KCN1 also downregulated transcription of endogenous HIF-1 target genes, such as *VEGF*, *Glut-1*, and *carbonic anhydrase 9*, in a hypoxia-responsive element (HRE)-dependent manner. KCN1 potently inhibited the growth of subcutaneous malignant glioma tumor xenografts with minimal adverse effects on the host. It also induced a temporary survival benefit in an intracranial model of glioma but had no effect in a model of melanoma metastasis to the brain. Mechanistically, KCN1 did not downregulate the levels of HIF-1α or other components of the HIF transcriptional complex; rather, it antagonized hypoxia-inducible transcription by disrupting the interaction of HIF-1α with transcriptional coactivators p300/CBP.

Conclusions: Our results suggest that the new HIF pathway inhibitor KCN1 has antitumor activity in mouse models, supporting its further translation for the treatment of human tumors displaying hypoxia or HIF overexpression. *Clin Cancer Res; 1–11. ©2012 AACR.*

Introduction

Hypoxia is a microenvironmental condition that is prevalent in solid tumor development, largely due to inadequate vascularization and rapid proliferation of tumor cells (1–3). To counter the detrimental effects of hypoxia, tumor cells activate a range of adaptive molecular mechanisms that play a critical role in all hallmarks of cancer (4). These include switching from oxidative phosphorylation to anaerobic glycolysis, angiogenesis, increased cell migration potential, and genetic alterations that prevent hypoxia-induced apoptosis. A family of heterodimeric transcription factors termed hypoxia-inducible factors (HIF) governs the primary transcriptional response to hypoxia. HIFs consist of one of HIF-1α, 2α, or 3α (the O_2-regulated subunits) and the constitutively expressed HIF-1β (5). Under normoxic conditions, α subunits are hydroxylated by a family of prolylhydroxylases, ubiquitylated in a Von Hippel-Lindau protein–dependent manner, and degraded in the proteasome (6). Under hypoxic conditions, α subunits are stabilized, translocate into the nucleus where they interact with the HIF-1β subunit, recruit co-activators p300/CBP, and

Authors' Affiliations: Departments of [1]Neurosurgery, [2]Hematology and Medical Oncology, and [3]Radiology and Imaging Sciences, and [4]Biostatistics & Bioinformatics Shared Resource, Emory University School of Medicine; [5]Winship Cancer Institute, Emory University, Atlanta, Georgia; [6]Department of Chemistry and The Skaggs Institute for Chemical Biology, The Scripps Research Institute; [7]Department of Chemistry and Biochemistry, University of California, San Diego, La Jolla, California; and [8]Department of Pharmaceutical Sciences, Cancer Biology Center, School of Pharmacy, Texas Tech University Health Sciences Center, Amarillo, Texas

Note: Supplementary data for this article are available at Clinical Cancer Research Online (http://clincancerres.aacrjournals.org/).

S. Yin and S. Kaluz contributed equally and should be considered joint first authors.

Current address for R.G. de Noronha: BIAL – Portela & C.[a] S.A., LIQ – DID, À Avenida da Siderurgia Nacional, 4745-457 S. Mamede do Coronado, Portugal.

Corresponding Author: Erwin G. Van Meir, Winship Cancer Institute, Emory University, 1365C Clifton Rd. N.E, C5078, Atlanta, GA 30322. Phone: 404-778-5563; Fax: 404-778-5550; E-mail: evanmei@emory.edu

doi: 10.1158/1078-0432.CCR-12-0861

Published OnlineFirst August 24, 2012; DOI: 10.1158/1078-0432.CCR-12-0861

Translational Relevance

Glioblastoma, one of the most aggressive and lethal cancers, with a life expectancy of less than 1 year, currently has no effective cure. The hypoxia-inducible factor-1 (HIF-1) plays a critical role in tumor adaptation to the hypoxic microenvironment and associates with poor prognosis and treatment failure. The HIF pathway plays a prominent role in glioblastoma, and targeting the HIF pathway has become an important therapeutic strategy. Here, we evaluate for the first time the anticancer activity of arylsulfonamide KCN1, the lead inhibitor in a novel class of small-molecule inhibitors of the HIF-1 pathway we recently discovered. Our results show that KCN1 displays potent antiglioma activity in a subcutaneous mouse model, whereas its activity was more limited in orthotopic brain tumor models. Arylsulfonamides thus have therapeutic potential for glioblastoma and other human tumors, although further optimization of their pharmacologic properties will be required.

regulate (HIF-1 and 2 positively, HIF-3 negatively) more than 100 target genes via binding to specific DNA sequences termed hypoxia-responsive elements (HRE; ref. 7).

CBP and p300 are homologous transcriptional coactivators, which act as a bridge linking DNA-binding transcription factors to the basal transcriptional machinery (8, 9). p300/CBP possess strong histone acetyltransferase activity that regulates remodeling of local chromatin structures and makes DNA more accessible to other regulators (8). The interaction between HIF-1α and p300/CBP, mediated by the C-terminal activation domain (CAD) of the former and the cysteine-histidine rich 1 (CH1) domain of the latter (10), is physiologically regulated via O_2-dependent hydroxylation of N803 in CAD by factor inhibiting HIF-1 (FIH-1; ref. 6). Recently, a weaker interaction between the HIF-1α N-terminal activation domain and p300/CBP CH3 was also reported (11). The critical role of p300/CBP in HIF function has been established by showing that blockade of the HIF-1α–p300/CBP interaction markedly attenuated HIF activity (12).

The close relation of HIF-activated gene products with tumor progression/metastasis identifies HIF as an attractive therapeutic target. Previous studies have established that inhibition of the HIF pathway can inhibit malignant characteristics in a number of cancers (13, 14), and several small-molecule inhibitors of HIF signaling have already been described (15–19). In addition, many anti-cancer compounds used in the clinic or in preclinical development were found to inhibit the HIF pathway indirectly (20–24). Despite this, new inhibitors of the HIF pathway, preferentially with defined and/or novel mechanism of action, need to be identified, and it is currently too early to determine which agent will have the best antitumor efficacy and safety profile.

To identify novel chemotypes with anti-HIF pathway activity, we previously conducted a cell-based screen to identify small-molecule inhibitors of HIF transcriptional activity in a combinatorial library (>10,000 compounds) built upon a 2,2-dimethyl-2*H*-chromene scaffold (25). In this library, we have identified arylsulfonamides as a novel chemotype with high nano-to-low micromolar (IC_{50}) HIF-inhibitory activity (26). Here, we show that the lead compound identified in the screen, 3,4-dimethoxy-*N*-[(2,2-dimethyl-2*H*-chromen-6-yl)methyl]-*N*-phenylbenzenesulfonamide (KCN1) inhibits HIF transcriptional activity through the disruption of the interaction between the HIF-1α subunit and transcriptional coactivators p300/CBP. Moreover, we show that KCN1 has significant potential for further development as a therapeutic as it strongly suppresses the growth of malignant glioma cells *in vivo* without any significant toxicity.

Materials and Methods

KCN1 synthesis and formulation for *in vivo* delivery

We generated KCN1 using a 4-step synthesis described in Supplementary Fig. S1A, and its structure was confirmed by UV, infrared (IR), mass spectroscopy (MS), and NMR spectroscopy (not shown). For cell culture experiments, a 10 mmol/L stock solution of KCN1 in dimethyl sulfoxide (DMSO) was diluted in pre-warmed media. For animal experiments, we developed a formulation for the delivery of KCN1 by preparing a stock solution (12 mg/mL) in a 1:1 mix of 200 proof ethanol and Cremophor EL (Sigma cat # C5135-500G) by vortexing and heating to 80°C to 90°C in a water bath. Before intraperitoneal (i.p.) administration, the KCN1 stock solution was diluted 1:5 with sterile PBS to a final concentration of 2.4 mg/mL and rapidly administered to avoid precipitation.

Cell culture

The human glioblastoma cell lines (LN229, U251MG, D54MG, D645MG, and LN443) and their growth conditions were previously described (27). The cells were routinely tested for mycoplasma, but no genetic authentication was conducted. LN229HRE-luc/lacZ cells were generated by stably transfecting LN229 cells with a bidirectional reporter construct (pBIGL-V6R) in which the firefly *luciferase* and *LacZ* reporter genes are under the control of 6 head to tail tandem copies of the *VEGF* HRE in rightward orientation (clone LN229V6R#18; Hygro selection 600 μg/mL; ref. 22). LN229CMV-luc and LN229CMV-lacZ cells were made by stably transfecting CMV promoter-luciferase (CMV-pGL2basic) or CMV promoter-β-galactosidase (CMV-pLacZ) reporters in LN229 cells using G418 (600 μg/mL) selection. Stably transfected cells were maintained in media with appropriate selection agents. Cells were pretreated with KCN1 or 1% DMSO (final concentration in media) vehicle control for 1 hour under normoxia (21% O_2); then incubation continued under normoxia or hypoxia (1% O_2) using a hypoxia incubator (Thermo Forma model 3130). KCN1 exhibited significant chemical stability, as high-

Published OnlineFirst August 24, 2012; DOI: 10.1158/1078-0432.CCR-12-0861

performance liquid chromatography (HPLC) analysis confirmed that it is structurally intact when incubated at 37°C for up to 27 hours in cell culture (Supplementary Fig. S2).

Plasmids and transient transfection assays

The *VEGF* promoter construct was prepared by cloning the [−1,181; +95] *VEGF* gene fragment (numbers are relative to transcription start site, Accession No. AF 095785) in the pGL2basic vector (Promega). The [−173; +31] *carbonic anhydrase 9* (*CA9*) promoter constructs were described previously (28). The *CA9* and *VEGF* HRE mutant promoter constructs contain the ATGCACGTA to ATGCTTTTA [−11; −3] (28) and TACGTGGGC to TAAAAGGGC [−975; −967] mutations, respectively. pNF-κB-luc and pAP1-luc vectors were from Stratagene, p53-responsive PG13PyLuc was described earlier (29). Promoter constructs or the pBIGL-V6R construct were cotransfected with the *Renilla* luciferase expressing pRL-CMV (internal control for transfection efficiency) using the Effectene Transfection Reagent (Qiagen). Cells were exposed to the transfection mixture for 16 hours, trypsinized, plated at 40,000 cells/cm^2, and allowed to adhere for 5 hours. The cells were then pretreated with 10 μmol/L KCN1 or 1% DMSO (final concentration in medium) for 1 hour and exposed to normoxia or hypoxia for 24 hours in the presence of inhibitor.

Reporter assays

Firefly and *Renilla* luciferase activities were measured with a Dual-Luciferase Reporter Assay System (Promega) in a 20/20^n Luminometer (Promega). Promoter activities were expressed as the average ratios of firefly to *Renilla* luciferase activities (±SD) from at least 3 independent experiments carried out in triplicates. Firefly luciferase activity in lysates of LN229HRE-luc/LacZ xenograft sections was similarly measured and normalized against protein concentration. For β-galactosidase staining, cells were fixed in 1× PBS containing 0.5% glutaraldehyde, 1.25 mmol/L EGTA, and 2 mmol/L $MgCl_2$ for 5 minutes, washed 3 times with 0.1 mol/L sodium phosphate, pH 7.3, 2 mmol/L $MgCl_2$, 0.01% deoxycholate, and 0.02% NP-40 for 5 minutes, stained in washing buffer supplemented with 1 mg/mL X-gal, 5 mmol/L potassium ferrocyanide, and 5 mmol/L potassium ferricyanide for 4 hours, and stored in washing buffer.

Northern blot analysis

Total cellular RNA was extracted in TRIzol (Fisher), separated by electrophoresis in 1% agarose-formaldehyde gels, and transferred to a nylon membrane (GE Healthcare). *VEGF*, *Glut1*, and *β-actin* mRNA levels were analyzed as previously described (22).

Reverse transcriptase-PCR analysis

Total RNA was isolated with an RNeasy mini kit (Qiagen) and cDNA, synthesized with a ProtoScript first-strand cDNA synthesis kit (New England Biolabs), was amplified with *Angiopoietin-like 4* (*Angptl4*; GCCTATAGCCTGCAGCTCAC sense and AGTACTGGCCGTTGAGGTTG antisense), *CA9* (CTGTCACTGCTGCTTCTGAT sense and TCCTCTCCAGGTAGATCCTC antisense), *VEGF* (CCTTGCTGCTCTACCTCCAC sense and CACACAGGATGGCTTGAAGA antisense), and *β-actin* (ACAACGGCTCCGGCATGTGCAA sense and CGGTTGGCCTTGGGGTTCAG antisense) primer pairs as described previously (28).

VEGF ELISA

VEGF concentrations in cell media or lysates of frozen tumor sections were determined with an ELISA kit (R&D Systems) as recommended and normalized against protein concentrations.

Western blot analysis

Total cell lysates from control and KCN1-treated LN229 cells were separated by SDS-PAGE and probed with anti–HIF-1α (1:600; BD Bioscience), anti–HIF-1β (1:1,000; BD Bioscience), anti–CAIX (1:1,000; Novus Biologicals), anti–β-actin (1:1,000; Santa Cruz Biotechnology), and anti–histone H1 (1:1,000; Santa Cruz Biotechnology) antibodies as previously described (22).

Pull-down of the HIF complex with an HRE oligonucleotide

Nuclear extracts, prepared with the NE-PER kit (Pierce), were incubated with a 5′-biotinylated double-strand oligonucleotide comprising two *VEGF* HRE motifs (underlined; 5′-CCACAGTGATACGTGGGCTCCAACAGGTCCTCTTC-CACAGTGATACGTGGGCTCCAACAGGTCCTCTT-3′) in a buffer A [10 mmol/L Tris, pH 8.0, 150 mmol/L NaCl, 12% glycerol, 1 mmol/L dithiothreitol (DTT)] at room temperature for 20 minutes. Prewashed streptavidin agarose beads (Pierce) were then added to the samples, incubated with agitation overnight at 4°C, recovered by centrifugation, and washed 4 times with buffer A. Pulled down proteins were detached from the beads by denaturation in a SDS sample buffer (50 mmol/L Tris, pH 6.8, 2% SDS, 10% glycerol, 0.02% bromophenol blue, 1 mmol/L DTT), separated by SDS-PAGE, and HIF-1α and p300 proteins were detected by immunoblotting.

Coimmunoprecipitations

Nuclear extracts were prepared from cells recovered by scraping in ice-cold PBS, and aliquots (0.5 mg) were incubated with 2 μg of a primary antibody and protein G sepharose beads (Amersham) at 4°C overnight. Beads were recovered by centrifugation, extensively washed with 50 mmol/L Tris, pH 8.0, 150 mmol/L NaCl, 1% NP-40, 1 mmol/L DTT, and protease inhibitors (EDTA-free Complete, Roche). Samples were denatured in the SDS sample buffer, separated by SDS-PAGE, and antibodies against HIF-1α, HIF-1β, p300 (1:1,000; Santa Cruz), CBP (1:1,000; Abcam), and histone H1 proteins were used for immunoblotting.

Chromatin immunoprecipitation assay

Chromatin immunoprecipitation (ChIP) assays were conducted with the EZChIP Assay Kit (Cell Signaling

Published OnlineFirst August 24, 2012; DOI: 10.1158/1078-0432.CCR-12-0861

Technology). A total of 4×10^7 cells were pretreated with 1% DMSO (control) or 10 μmol/L KCN1 for 1 hour, transferred to hypoxia for 24 hours, and fixed in 1% formaldehyde at room temperature for 20 minutes. Isolated nuclei were lysed, followed by chromatin digestion with micrococcal nuclease. Chromatin fragments were immunoprecipitated with anti-HIF-1α, anti-p300, or anti-CBP polyclonal antibodies as mentioned above or rabbit IgG as a control. After reversal of cross-linking and DNA purification, DNA from input (1:20 dilution) or immunoprecipitated samples was analyzed with PCR, and products were separated by 2% agarose gel electrophoresis. Primers used to detect endogenous *CA9* HRE were 5′-GACTTTGGCTCCATCTCTGC-3′ (sense) and 5′-GACAGCAGCAGTTGCCACAGT-3′ (antisense).

Animal experiments

In two independent experiments, LN229HRE-luc/lacZ cells (5×10^6) were injected subcutaneously (s.c.) into the flanks of *nu/nu* mice [athymic nude mice (Harlan), two dorsal injection sites/mouse] as described (30, 31), and the mice were randomized into vehicle control and KCN1 chronic treatment groups (8 mice per group in the first experiment and 15 mice per group in the repeat experiment). The mice received tattoos for easy identification (32). KCN1, prepared daily in ethanol/Cremophor EL (1:1) formulation, was administered at 60 mg/kg i.p. 5 d/wk for the duration of the experiment, starting 24 hours after tumor cell injection. Tumor volumes were measured weekly as described (32), and animals were sacrificed as per Institutional Animal Care and Use Committee (IACUC) guidelines and the tumors harvested. Sections of frozen tumors, prepared with a cryostat (Leica CM 1850), were mounted on glass slides, and lysed in 100 μL of 1× Passive Lysis Buffer (Promega) for measurement of luciferase activity and VEGF protein levels. For the evaluation of acute KCN1 effects on hypoxia-inducible genes by RT-PCR, tumors were pre-established for 10 weeks to a size of approximately 300 mm^3, when a single dose of KCN1 was administered. Animals were sacrificed 12 hours later, and tumors harvested and frozen for subsequent RNA analysis.

For the intracranial experiments, *nu/nu* athymic mice and C57BL/6 mice were stereotactically inoculated with 1×10^6 LN229HRE-luc/lacZ or LN229CMV-luc and 5×10^4 B16LS9 cells, respectively, as described previously (31). KCN1 treatment started on day 10 (LN229 cells) or day 1 (B16LS9 cells) as described above. For the survival analysis, the Kaplan–Meier method was used to generate survival curves. The log-rank test was used to test the difference in the survival times of different groups.

Quantitative and statistical analysis

Densitometric scanning was conducted with ImageJ software. Data were analyzed using 2-sample *t* test (MS Office Excel 2007). Statistical comparisons of *in vivo* s.c. tumor growth were conducted by XenoCat_1.0_3 R package using a categorizing mixed-effects model (33). Differences between control and drug-treated tumor volumes were considered significant when $P < 0.05$. *, $P < 0.05$; **, $P < 0.01$; ***, $P < 0.001$.

Results

KCN1 inhibits HIF-inducible gene expression

Following the screening of a combinatorial library for inhibitors of HIF transcriptional activity, we identified KCN1 (Fig. 1A) as one of the most potent compounds (26, 34–36). KCN1 inhibited hypoxia-induced expression of luciferase in human glioma cells (LN229HRE-luc/lacZ cells) stably transfected with a hypoxia-inducible dual luciferase/β-galactosidase reporter pBIGL-V6R (22) in a dose-dependent manner, with an IC_{50} of approximately 590 nmol/L, whereas it had little effect on constitutive luciferase activity in LN229CMV-luc cells (Fig. 1B, left). Similarly, KCN1 inhibited hypoxia-induced β-galactosidase expression in LN229HRE-luc/lacZ cells but not the constitutive expression in control LN229CMV-lacZ cells (Fig. 1B, right). The ability of KCN1 to inhibit HRE-dependent reporter activity was observed in a genetically diverse set of glioblastoma cell lines (U251MG, D54MG, D645MG, and LN443) as shown by transient transfection with the pBIGL-V6R reporter plasmid (ref. 37; Fig. 1C), indicating that KCN1 is a general inhibitor of HIF transcription in gliomas. KCN1 was not a broad inhibitor of transcription, as reporters for NF-κB [5 response elements (RE)], AP1 (6 RE), and p53 (13 RE) transcription factors were not affected (Fig. 1D). KCN1 did not affect cell viability at concentrations below 100 μmol/L in LN229 cells (35, 36), further ruling out the possibility that the inhibitory effect on HRE-driven expression was due to nonspecific cytotoxicity. *In vitro* testing in the NCI-60 Tumor Cell Line Screen confirmed that at 10 μmol/L, KCN1 did not significantly inhibit the growth of most cell lines, except for non–small cell lung cancer, melanoma, and leukemia cell lines (Supplementary Fig. S3).

Next, we tested whether KCN1 inhibits the endogenous target genes of HIF-1. First, we probed levels of *VEGF*, *Glut1*, and *CA9* mRNAs in glioma cells by Northern blotting and reverse transcriptase (RT)-PCR. Compared with the vehicle controls, KCN1 significantly reduced hypoxia-induced levels of these transcripts, whereas it had no effect on *β-actin* mRNA (Fig. 2A). VEGF ELISA revealed that hypoxia potently activates the secretion of VEGF by LN229 cells and this was antagonized by KCN1 (Fig. 2B, left). Transcriptional activity of a wild-type (wt; but not HRE-mutant) *VEGF* promoter–driven reporter was also significantly upregulated by hypoxia and inhibited by KCN1 in LN229 cells (Fig. 2B, right). Immunoblotting confirmed that expression of CA9 was also downregulated by KCN1 (Fig. 2C, left). Hypoxia-activated expression from the reporter construct containing the wt *CA9* promoter was also inhibited, albeit to a lesser extent than the one driven by the *VEGF* promoter (Fig. 2C, right). Acute KCN1 treatment also inhibited expression of endogenous hypoxia-inducible genes *in vivo* in pre-established xenografts of LN229HRE luc/lacZ cells (Fig. 2D). Together,

Published OnlineFirst August 24, 2012; DOI: 10.1158/1078-0432.CCR-12-0861

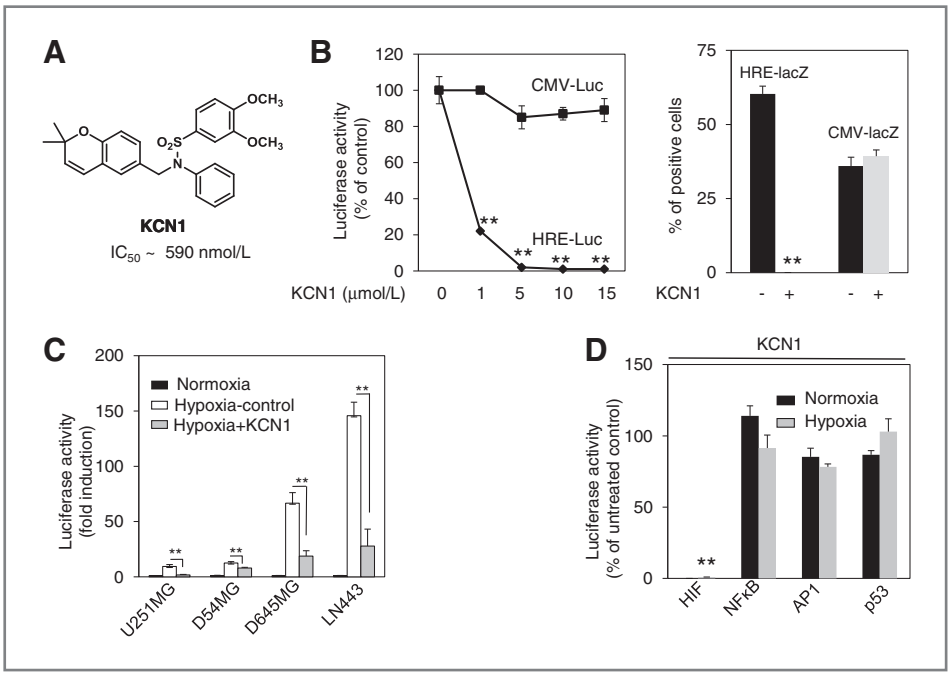

Figure 1. KCN1 specifically inhibits hypoxia-inducible gene expression driven by exogenous HRE-reporter constructs in glioma cells. A, chemical formula of KCN1 and IC_{50} established in a cell-based assay using LN229HRE-luc/LacZ cells with a stably integrated hypoxia-responsive luciferase reporter. $N = 21$ independent experiments carried out in triplicate. B, left, KCN1 inhibits hypoxia (1% O_2)-induced luciferase activity in LN229HRE-luc/lacZ (HRE-luc) but not in LN229CMV-luc (CMV-luc) cells. Data from 3 independent experiments ($n = 3$) carried out in triplicate are expressed as percent of the control activity (1% DMSO; ±SD). **, $P < 0.01$. Right, KCN1 inhibits hypoxia (1% O_2)-induced β-galactosidase activity in LN229HRE-luc/lacZ but not in LN229CMV-lac Z cells. β-Galactosidase activity was detected by chemical staining and positive cells were quantified. C, KCN1 inhibits hypoxia-inducible gene expression in other glioma cell lines. Cell lines were transiently cotransfected with pBIGL-V6R-HRE-luc construct and pRL-CMV and tested under normoxia or hypoxia (1% O_2) ± KCN1 (10 μmol/L). Average of the ratio of luciferase and *Renilla* activities (±SD) from 3 independent experiments ($n = 3$) carried out in triplicate was calculated, and promoter activities are expressed as fold induction over the normoxic control set as 1. **, $P < 0.01$. D, KCN1 (10 μmol/L) inhibits the activity of a HIF-activated luciferase reporter construct, but not that of reporters for other transcription factors. Constructs were transiently transfected with pRL-CMV in LN229 cells and tested under normoxia or hypoxia (1% O_2). Data from 3 independent experiments ($n = 3$) carried out in triplicate are expressed as percent of the vehicle-treated controls (1% DMSO; ±SD). **, $P < 0.01$.

these data show that KCN1 inhibits expression of representative endogenous hypoxia-inducible genes that encode regulators of important tumor functions such as angiogenesis, glucose transport, and cellular pH.

KCN1 is antitumorigenic *in vivo*

To assess the antitumor potential of KCN1, we examined its anti-glioma activity in *in vivo* animal models. LN229HRE-luc/lacZ cells were inoculated s.c. into both flanks of *nu/nu* mice and treated i.p. with KCN1 (60 mg/kg) or vehicle 5× per week. Cumulative data from 2 independent experiments show that after a 10-week chronic treatment period, the average tumor volume in KCN1-treated animals was more than 4-fold lower than that in the controls (Fig. 3A). Remarkably, 10 of 42 tumors in the KCN1 group grew till about 20 to 60 mm^3 after 4 to 6 weeks and then completely regressed. Six more tumors showed stable disease at tumor sizes of 20 to 170 mm^3. When grouped, the dissected tumors in both experiments revealed an approximately 3-fold weight difference between the groups (Fig. 3B and C). Finally, the average tumor growth rates measured were also found to be significantly lower in the KCN1-treated group than in the control group (Fig. 3C). KCN1 was further tested in a s.c. model where tumors were allowed to form for 3.5 weeks (~26 mm^3) before the treatment started. Tumor growth curves in Supplementary Fig. S4 indicate that KCN1 shows significant antitumor activity in pre-established tumors, although it was most potent as a cancer prevention agent. KCN1 was also antitumorigenic in animal models of pancreatic cancer (38) and uveal melanoma and its metastasis to the liver (70% reduction of tumor size in the eye and 50% reduction in number of hepatic metastases; manuscript in preparation). KCN1 injections were well tolerated and did not evidence any signs of extraneous toxicity; the animals' behavior and activity were indistinguishable from untreated animals, and their bodily appearance and weight were normal (Supplementary Fig. S5). Initial pathologic examination of main organs showed no ultrastructural changes in brain, kidney, gastrointestinal tract, and lung (Supplementary Fig. S6). A treatment-related change was observed in the liver, where swelling was evidenced macroscopically at autopsy, and pathology showed tissue edema with bile duct stasis, yet without evidence for any hepatocyte death. The swelling was reversible within 2 to 3 weeks after treatment was discontinued (data not shown) and may be related to the Cremophor:ethanol formulation, which can interfere with hepatic blood flow (39, 40).

Published OnlineFirst August 24, 2012; DOI: 10.1158/1078-0432.CCR-12-0861

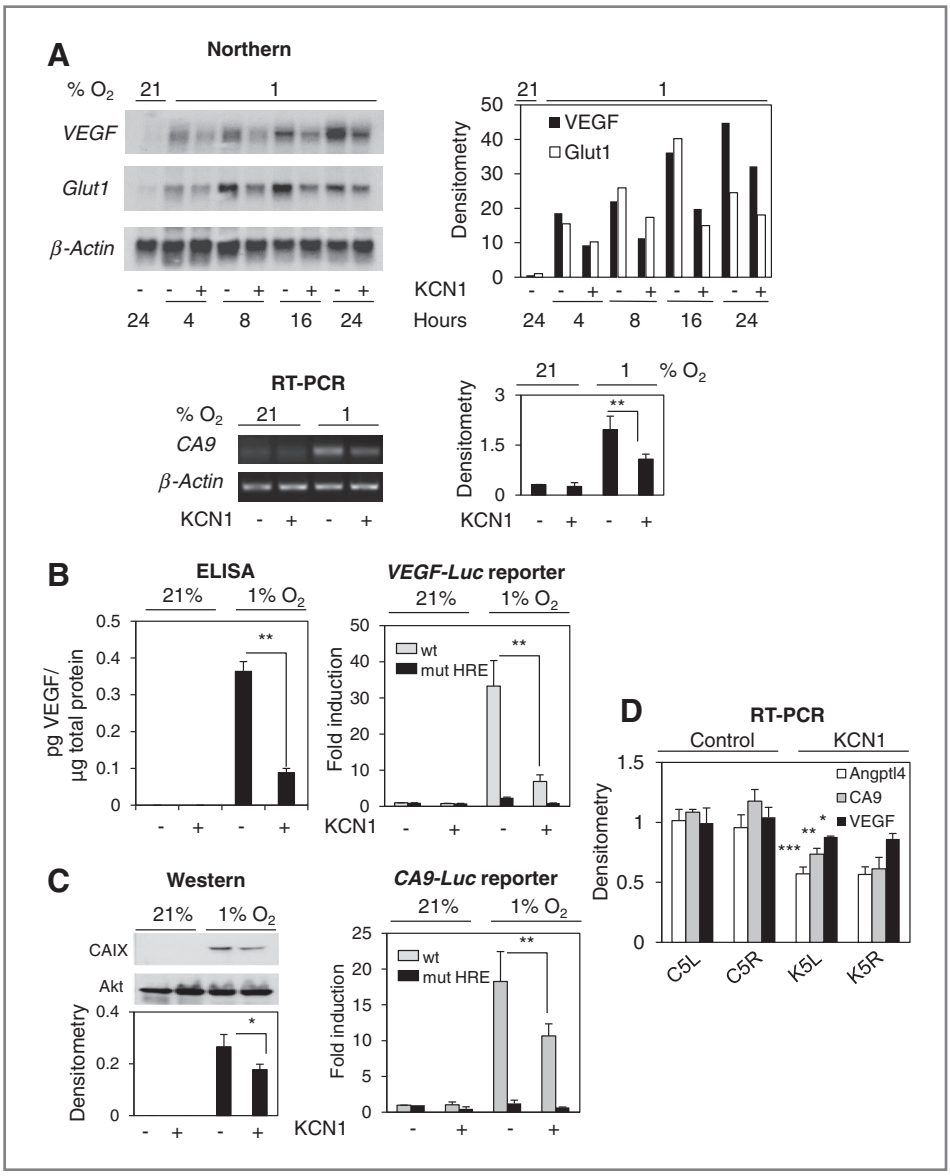

Figure 2. KCN1 inhibits the expression of endogenous hypoxia-inducible genes. A, left, Northern blot analysis of *VEGF* and *Glut-1* gene expression in LN229 cells under normoxia and hypoxia (1% O_2) ± KCN1 (25 µmol/L) treatment for 4 to 24 hours. β-Actin was used as a loading control. Right, densitometric analysis of the Northern blot. Data are expressed as the ratio of *VEGF*(*Glut1*)/*β-actin* signal. Bottom left, RT-PCR analysis of *CA9* and *β-actin* gene expression with and without KCN1 (25 µmol/L) treatment in U251MG cells. Right, relative *CA9* expression levels were quantified by densitometry and normalized against *β-actin* expression (average from 3 different gels ± SD). B, left, ELISA-mediated detection of VEGF levels in the 48-hour conditioned media of LN229 cells grown under normoxia (21% O_2) or hypoxia (1% O_2) ± KCN1 (10 µmol/L) treatment. Right, activity of *VEGF* promoter constructs with wt or mutant HRE in transiently transfected LN229 cells ± KCN1 (10 µmol/L). A constitutively active CMV-*Renilla* luciferase construct was cotransfected as a control. Average of the ratio of luciferase and *Renilla* activities (±SD) from 3 independent experiments ($n = 3$) carried out in triplicate was calculated and promoter activities are expressed as fold induction over the normoxic control set as 1. C, left, Western blot mediated detection of CA9 expression in LN229 cells under normoxia or hypoxia ± KCN1 (10 µmol/L). Akt expression was used as a loading control. Relative CA9 expression levels were quantified by densitometry and normalized against Akt expression (average from 2 different blots ± SD). Right, activity of *CA9* promoter constructs with wt or mutant HRE in transiently transfected LN229 cells ± KCN1 (10 µmol/L). Normalization to the CMV-*Renilla* luciferase reporter was done as in B. **, $P < 0.01$; *, $P < 0.05$. D, relative *Angptl4*, *CA9*, and *VEGF* mRNA expression levels in control (vehicle) and KCN1-treated LN229HRE-luc/lacZ tumors analyzed by RT-PCR. Mice with pre-established s.c. LN229HRE-luc/lacZ tumors received a single dose of KCN1 (60 mg/kg i.p.) and the tumors were excised 12 hours later. Intensity of each *Angptl4*, *CA9*, *VEGF*, and *β-actin* band in agarose electrophoresis was quantified by densitometry and expression of hypoxia-inducible genes was normalized against *β-actin* expression (average from 3 different RT-PCR experiments ± SD). Results on tumors from 2 vehicle-treated (C5L, C5R) and 2 KCN1-treated (K5L and K5R) animals are shown. *P* values for *Angptl4*, *CA9*, and *VEGF* expression in control and KCN1-treated tumors were 0.000145, 0.00263, and 0.03042, respectively.

To gain an insight whether the tumors that did not regress after the 10-week KCN1 treatment period might have become resistant to the anti-HIF activity of KCN1, we analyzed the tumors for production of luciferase from the HIF-inducible reporter and endogenous VEGF in the drug- and vehicle-treated groups. Although tumor-to-tumor

Published OnlineFirst August 24, 2012; DOI: 10.1158/1078-0432.CCR-12-0861

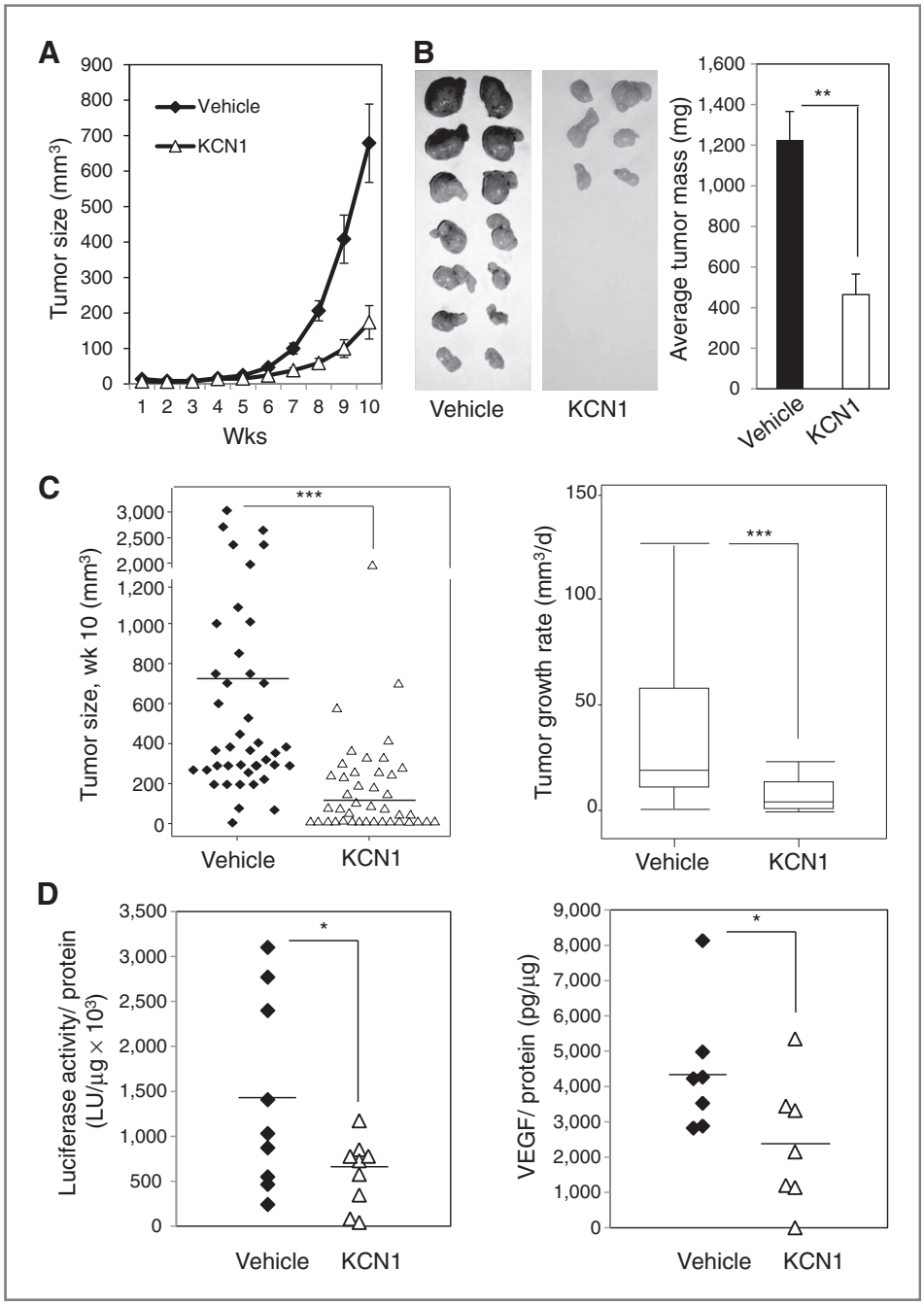

Figure 3. KCN1 inhibits the growth of malignant human glioblastoma xenografts, HRE activity, and VEGF levels *in vivo*. Nude mice carrying LN229HRE-Luc/LacZ cells (s.c. in the flanks; 2 tumors per mouse) were treated i.p. 5 d/wk with 60 mg/kg KCN1 in 1:1 ethanol/Cremophor (controls vehicle only). A, tumor volume. The growth curve shown is the combined result of 2 independent experiments. The first was conducted with 8 mice per group and the second with 15 mice per group. Average tumor size in each group (±SE) is shown. $P < 0.001$. B, size (left) and mass (right) of tumors excised from the first experiment (2 tumors per mouse). **, $P < 0.01$. C, left, individual tumor sizes of both experiments combined. Right, kinetics of tumor growth from week 9 to 10 expressed as increase in tumor size per day. ***, $P < 0.001$. D, left, effect of KCN1 on HRE-luciferase activity in tumors after 10 weeks of KCN1 treatment. Luciferase activity was measured in lysates of frozen tumor sections and normalized against protein concentration. *, $P = 0.017$. Right, VEGF levels in tumors after 10 weeks of KCN1 treatment. VEGF protein in lysates of frozen tumor sections was detected by ELISA and normalized against protein concentration. *, $P = 0.014$.

variation in luciferase activity and VEGF levels in each group was observed, the average values in both cases were still significantly lower ($P < 0.05$) in KCN1-treated tumors (Fig. 3D), confirming that in these resilient tumors, KCN1 is still inhibiting HIF activity and VEGF production to some extent.

We then tested whether KCN1 would show efficacy in orthotopic brain tumors. We used two intracranial tumor models: one with LN229 human glioma cells in athymic *nu/nu* mice and the other with B16LS9 mouse melanoma cells in syngeneic C57BL/6 mice. KCN1 treatment temporarily reduced mortality rate in mice injected with LN229 cells (significance for days 41–48 was $P < 0.05$ and for days 42–47 $P < 0.01$), although the survival endpoint showed no difference between the groups (Supplementary Fig. S7A and S7B). No survival benefit was observed in the more aggressive B16LS9 melanoma model (Supplementary Fig. S7C).

We further determined whether KCN1 showed blood–brain barrier (BBB) permeability, using *in vitro* BBB assays with 14C*-labeled KCN1 (41). Measuring of apical to basolateral brain endothelial cell permeability revealed that KCN1 has a permeability coefficient comparable with

Published OnlineFirst August 24, 2012; DOI: 10.1158/1078-0432.CCR-12-0861

mannitol, a cell-impermeable control (Supplementary Fig. S8). Our pharmacokinetic studies found that the concentration of KCN1 in brains of CD1 mice (~0.4 μmol/L) was at least 5× lower than in other organs (spleen, kidney, liver, lung) after i.p. and intravenous administration (38). Together, these data are indicative of the absence of an active influx mechanism for KCN-1, suggesting that it may not penetrate an intact BBB efficiently.

Collectively, these findings provide proof-of-principle for the antitumor efficacy, inhibition of HIF activity *in vivo*, and low toxicity of KCN1 and provide the basis for further preclinical development of this class of agents. Chemical modifications to increase their potency, optimize their pharmacology, and enable their BBB permeability are still warranted.

KCN1 does not decrease levels of components of the HIF-1 complex

To characterize the molecular mechanism of inhibition of HIF-1–dependent transcription, we initially examined the effect of KCN1 on levels of components of the HIF-1 complex. Western blot analysis of total cell lysates from LN229 cells revealed that over the 12- to 48-hour treatment period, the HIF-1α protein levels showed little variation in response to KCN1 (Fig. 4A). Other constituents of the HIF-1 complex (HIF-1β and p300) were also unaffected by KCN1 treatment. Similar results were obtained with other cell lines (U87MG, HEK293ft) in which KCN1 had been shown to inhibit HRE activity (data not shown). These observations establish that KCN1 does not inhibit HIF activity by down-regulating the levels of components of the HIF-1 transcriptional complex.

KCN1 prevents the binding of transcriptional cofactors p300 and CBP on the HRE sequence *in vitro* and *in vivo*

We next interrogated how KCN1 affects the assembly of a functional HIF-1 transcriptional complex on an HRE sequence using a DNA–protein *in vitro* pull-down experiment. A biotinylated double-strand oligonucleotide with two copies of the *VEGF* HRE sequence was exposed to nuclear extract from hypoxic glioma cells and pulled-down complexes analyzed by immunoblotting for the presence of p300 and HIF-1α (Fig. 4B). The input fractions confirmed that KCN1 does not affect HIF-1α and p300 levels, and analysis of the pulled down fractions showed that the HRE-binding activity of HIF-1α is not compromised by KCN1. In contrast, KCN1 decreased the amount of HRE-bound p300 in a dose-dependent manner, hinting that KCN1 may prevent the recruitment of the p300 cofactor to the pre-assembled HRE–HIF-1 complex. To further establish whether KCN1 prevents the recruitment of p300 and CBP to the chromatin of an endogenous hypoxia-inducible gene *in vivo*, we studied the assembly of the individual protein components of the HIF complex on the *CA9* gene HRE by ChIP assay. ChIP data indicated that KCN1 had no effect on the binding of HIF-1α to the *CA9* HRE DNA sequence, corroborating the conclusion from the pull-down experiment that KCN1 does not affect HRE-binding activity of HIF-1. Consistent with the pull-down assays, the levels of

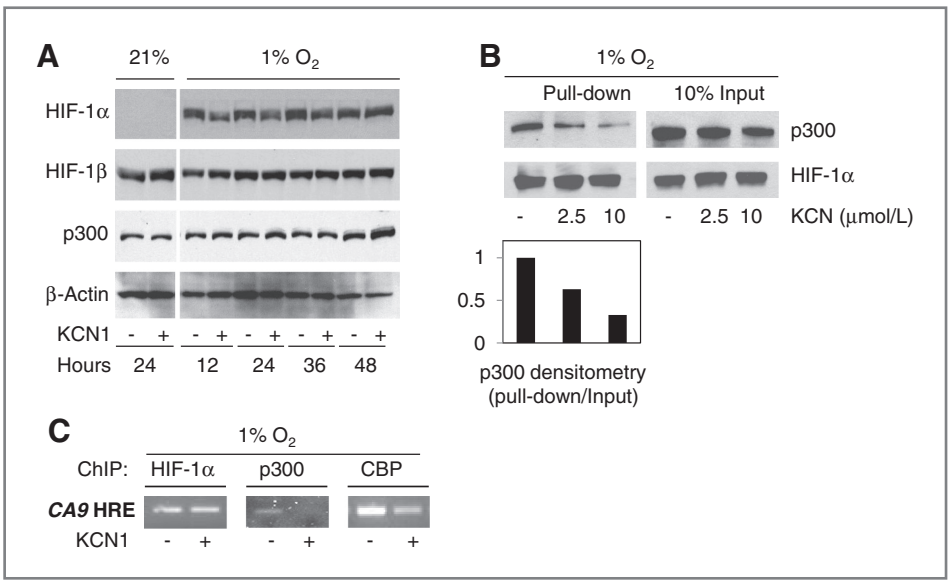

Figure 4. The mechanism of action of KCN1 involves the disruption of the HIF-1α, HIF-1β, p300/CBP transcription complex. A, Western blot analysis of whole-cell lysates shows that KCN1 (25 μmol/L) treatment does not significantly alter the levels of the HIF-1α, HIF-1β subunits, or of the p300 transcription cofactor in hypoxic (1% O_2) LN229 cells over a 12- to 48-hour time frame. B, pull-down experiments show that KCN1 reduces the interaction between p300 and the HRE sequence. Top, a biotinylated HRE probe was incubated with LN229 nuclear extract, complexes were pulled down with streptavidin–agarose beads and tested for the presence of HIF-1α and p300 by Western blotting. Bottom, densitometric analysis of the p300 pull-down. Data are expressed as the ratio of p300 pull-down signal/p300 input signal. C, ChIP analysis shows a reduction in the binding of p300 and CBP cofactors on the *CA9* HRE by KCN1 (10 μmol/L) in LN229 cells, whereas that of HIF-1α was unaffected.

Published OnlineFirst August 24, 2012; DOI: 10.1158/1078-0432.CCR-12-0861

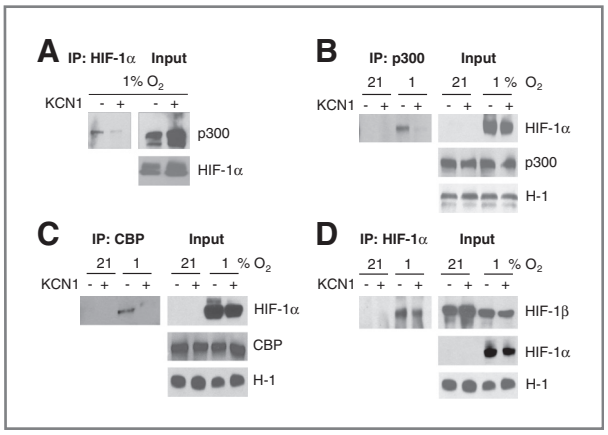

Figure 5. KCN1 disrupts the HIF-1α, HIF-1β, p300/CBP transcription complex. Co-IP in cell extracts of LN229 cells pretreated with KCN1 (25 μmol/L) shows a reduction in binding between HIF-1α and p300/CBP cofactors. A Western blot analysis on the cell extract was conducted as a control for equal protein distribution (input). H-1, Histone H-1. A, co-IP of p300 with HIF-1α; B, co-IP of HIF-1α with p300; C, co-IP of HIF-1α with CBP; D, co-IP of HIF-1β with HIF-1α.

p300 and CBP were decreased in the complex assembled on the *CA9* HRE of KCN1-treated cells under hypoxia (Fig. 4C).

KCN1 interferes with the binding of HIF-1α to the transcriptional coactivators p300 and CBP

To more directly examine how KCN1 inhibits HIF-1α–p300/CBP assembly on the HRE, we conducted coimmunoprecipitation (co-IP) experiments. Both the co-IP of p300 with an HIF-1α antibody and the reversed co-IP of HIF-1α with a p300 antibody showed that KCN1 interferes with the HIF-1α–p300 interaction (Fig. 5A and B). Similarly, a co-IP with an antibody against the p300 paralog, CBP, also showed that the HIF-1α–CBP interaction is negatively affected by KCN1 (Fig. 5C). On the other hand, KCN1 had no appreciable effect on the HIF-1α–HIF-1β heterodimer formation (Fig. 5D).

Combined, the ChIP, HRE pull-down and co-IP assays support the notion that the mechanism of inhibition of HIF activity by KCN1 involves interference with HIF-1α–p300/CBP interaction, which causes p300/CBP deficiency in the HIF complex.

Discussion

A growing body of evidence supports the facilitating role of HIF and HIF-regulated gene products in tumor progression/metastasis; therefore, HIF is increasingly considered an attractive therapeutic target. The rationale for targeting HIF in cancer is that HIF is the key transcription factor responsible for the transactivation of a wide array of genes, many of which enhance survival and spread of tumor cells (13, 14). Blocking of HIF function would thus be expected to interfere with multiple attributes of tumor cells and eventually lead to tumor regression. Not surprisingly, significant effort and resources have been invested into identifying small molecules that would potently and specifically inhibit HIF.

Our laboratory has had a long-standing interest in the HIF pathway and the development of novel experimental therapeutics targeting the hypoxic status of tumors (22, 23, 37, 42–46). To identify new inhibitors of the HIF pathway, we have developed a cell-based assay as this format is more likely to yield pharmaceutically viable leads (47). The screen of a combinatorial library of natural product-like compounds (25) yielded a novel class of agents (arylsulfonamides) that inhibited HIF activity at high nano- to-low micromolar concentrations (26). Here, we showed that the initial lead compound in this class, KCN1, displayed inhibition of HIF-dependent expression in the context of artificial HRE enhancers as well as HREs in the endogenous HIF-inducible genes. Inhibition was dependent on the presence of a functional HRE, as evidenced by differential effects of KCN1 on wt-and HRE mutant *VEGF* and *CA9* promoter constructs. More importantly, KCN1 displayed significant antitumor activity *in vivo*. Systemic administration of KCN1 to mice harboring s.c. malignant gliomas markedly inhibited tumor growth and HIF activity in tumors in the absence of any significant toxicities even when the compound was administered daily at 60 mg/kg for extended periods of time. While some liver swelling was noticed at autopsy, this was reversible and likely linked to the use of Cremophor:ethanol (39, 40), suggesting that a new formulation or more soluble analogues need to be developed, a process we recently started with the synthesis of heteroarylsulfonamides (35, 36)

In contrast to the antitumor efficacy seen in s.c. cancer models, KCN1 showed a lesser therapeutic effect when tested in orthotopic brain tumor models (glioma and melanoma). Pharmacologic assessment of KCN1 distribution to the brain tumors and *in vitro* BBB permeability assays suggest that new analogues need to be developed with improved BBB permeability and biodistribution to the brain. Regulation of HIF-1 levels and activity is a complex multistep process, controlled primarily by HIF-specific factors, PHDs and FIH. In addition, HIF is situated at the convergence of major oncogenic signaling pathways [phosphoinositide 3-kinase (PI3K), mitogen-activated protein kinase (MAPK), mTOR] that indirectly activate the HIF pathway. Not surprisingly, the complexity of HIF regulation (transcription, translation, folding, transport, proteasomal degradation of HIF-α, DNA binding, and interaction with transcriptional coactivators) provides multiple steps that are "druggable," and small-molecule inhibitors intervening at various stages of the regulatory process have been identified (15, 20, 47, 48). A large number of agents initially developed to target signaling pathways, such as the inhibitors of PI3K, mTOR, MAPK, topoisomerase II, and even the modulators of microtubule dynamics, have been also shown to indirectly inhibit HIF-1 function (48). The search for new, more specific HIF inhibitors has already provided a number of novel agents: acriflavine, a specific inhibitor of HIF-1α–HIF-1β dimerization (16), and echinomycin and "programmable" polyamides that disrupt the interaction of HIF-1 with the HRE through DNA intercalation (49). Several of these agents are being

Published OnlineFirst August 24, 2012; DOI: 10.1158/1078-0432.CCR-12-0861

translated into clinical trials, whereas others have shown unacceptable toxicity. The difficulty in identifying compounds targeting the HIF-1α–p300/CBP interaction is underscored by a prior extensive chemical screen using a large library of 600,000 small molecules, which identified a single compound, chetomin, which displayed antitumor activity *in vivo*, albeit in the presence of some toxicity (12). Later work suggested that, rather than specifically targeting p300, chetomin chelates Zn^{2+} that is required for the structure and function of its CH1-3 domains (50).

In a cell-based assay, the molecular target(s) of an inhibitor is not immediately identified, and its identification can become a major challenge. Many of the prior reported HIF inhibitors, including 103D5R and KC7F2 we previously isolated (21, 22), suppress HIF function by reducing HIF-1α subunit levels. In contrast, we found that KCN1 does not appreciably alter the levels of HIF-1α, HIF-1β, or p300, suggesting that it may either affect the assembly or function of the HIF complex. We showed, using pull-downs, co-IPs, and ChIP, that KCN1 compromises interactions between HIF-1α and transcriptional coactivators p300/CBP, which impairs the recruitment of these cofactors to pre-assembled HRE–HIF complexes on the chromatin and prevents hypoxia-induced transcription. The interaction between HIF-1α and p300/CBP is mediated by the CAD of HIF-1α and the CH1 domain of p300/CBP (10) and to a lesser extent by the N-terminal activation domain of HIF-1α with the CH3 domain of p300/CBP (11) Our recent modeling studies evidenced putative binding sites for KCN1 on the CH1 domains of p300 and CBP, which are predicted to block the interaction with HIF-1α (41).

In summary, we have identified and characterized a novel type of HIF pathway inhibitor—a di-substituted sulfonamide with the naturally occurring 2,2-dimethyl-2*H*-chromene structural motif, designated KCN1. KCN1 inhibits HIF activity in an HRE-dependent cell-based assay with an IC_{50} of approximately 590 nmol/L and displays promising antitumor activity in animal models. KCN1 inhibits HIF function in a unique way, with the mechanism of action involving interference with HIF-1α–p300/CBP interactions (first-in-class), which results in coactivator deficiency in the HIF complex assembled on the target genes under hypoxia and in turn decreases transcription activity. Nonetheless, HIF-inhibitory activity may not be the only factor contributing to the antitumor effect of KCN1 and there could be other relevant targets. Further studies are warranted for translation of this promising chemotype toward clinical development, which include our ongoing structure–activity relationship studies directed toward improvement of potency and pharmacologic properties.

Disclosure of Potential Conflicts of Interest

E.G. Van Meir and K.C. Nicolaou have ownership interest as coinventors on patent owned by Emory University and Scripps. No potential conflicts of interest were disclosed by the other authors.

Authors' Contributions

Conception and design: S. Yin, S. Kaluz, A.A. Jabbar, R. Zhang, K.C. Nicolaou, E.G. Van Meir
Development of methodology: S. Yin, W. Wang, Z. Chen, R. Zhang, M.M. Goodman, E.G. Van Meir
Acquisition of data (provided animals, acquired and managed patients, provided facilities, etc.): S. Yin, N.S. Devi, A.A. Jabbar, J. Mun, Z. Zhang, P. R. Boreddy, T. Abbruscato, J.J. Olson, R. Zhang, M.M. Goodman, E.G. Van Meir
Analysis and interpretation of data (e.g., statistical analysis, biostatistics, computational analysis): S. Yin, S. Kaluz, W. Wang, Z. Wang, T. Abbruscato, Z. Chen, R. Zhang, E.G. Van Meir
Writing, review, and/or revision of the manuscript: S. Yin, S. Kaluz, R.G. de Noronha, Z. Wang, J.J. Olson, R. Zhang, M.M. Goodman, E.G. Van Meir
Administrative, technical, or material support (i.e., reporting or organizing data, constructing databases): E.G. Van Meir
Study supervision: R. Zhang, M.M. Goodman, E.G. Van Meir
Other: Chemical synthesis and characterization of KCN1, R.G. de Noronha; Conducted coimmunoprecipitations, pull-downs, ChIP, and promoter experiments, S. Yin, S. Kaluz; Designed and synthesized KCN1, K.C. Nicolaou, E.G. Van Meir; Conducted luciferase and mice s.c. tumorigenicity experiments, N.S. Devi; Conducted KCN1 pharmacokinetics in mice, W. Wang, R. Zhang; Synthesized [^{14}C]-KCN1, J. Mun, M.M. Goodman; Conducted BBB permeability studies, P.R. Boreddy, T. Abbruscato; Conducted mice intracranial experiments, A.A. Jabbar, Z. Zhang, J.J. Olson

Acknowledgments

The authors thank V. Belozerov for technical assistance.

Grant Support

This work was supported in part by the American Brain Tumor Association, the Brain Tumor Foundation for Children, the Charlotte Geyer Foundation, EmTechBio, the Southeastern Brain Tumor Foundation, the Emory University Research Council, the NIH (R01 CA116804, CA86335, and P30 CA138292), the V Foundation, the Max Cure Foundation, and the Samuel Waxman Cancer Research Foundation.

The costs of publication of this article were defrayed in part by the payment of page charges. This article must therefore be hereby marked *advertisement* in accordance with 18 U.S.C. Section 1734 solely to indicate this fact.

Received March 14, 2012; revised August 17, 2012; accepted August 18, 2012; published OnlineFirst August 24, 2012.

References

1. Kaur B, Khwaja FW, Severson EA, Matheny SL, Brat DJ, Van Meir EG. Hypoxia and the hypoxia-inducible-factor pathway in glioma growth and angiogenesis. Neuro-Oncology 2005;7:134–53.
2. Brat DJ, Castellano-Sanchez A, Kaur B, Van Meir EG. Genetic and biologic progression in astrocytomas and their relation to angiogenic dysregulation. Adv Anat Pathol 2002;9:24–36.
3. Tohma Y, Gratas C, Van Meir EG, Desbaillets I, Tenan M, Tachibana O, et al. Necrogenesis and Fas/APO-1 (CD95) expression in primary (de novo) and secondary glioblastomas. J Neuropathol Exp Neurol 1998;57:239–45.
4. Ruan K, Song G, Ouyang GL. Role of hypoxia in the hallmarks of human cancer. J Cell Biochem 2009;107:1053–62.
5. Huang LE, Bunn HF. Hypoxia-inducible factor and its biomedical relevance. J Biol Chem 2003;278:19575–8.
6. Kaelin WG Jr, Ratcliffe PJ. Oxygen sensing by metazoans: the central role of the HIF hydroxylase pathway. Mol Cell 2008;30:393–402.
7. Wenger RH, Stiehl DP, Camenisch G. Integration of oxygen signaling at the consensus HRE. Sci STKE 2005;2005:re12.
8. Iyer NG, Ozdag H, Caldas C. p300/CBP and cancer. Oncogene 2004;23:4225–31.
9. Kasper LH, Fukuyama T, Biesen MA, Boussouar F, Tong CL, de Pauw A, et al. Conditional knockout mice reveal distinct functions for the global transcriptional coactivators CBP and p300 in T-cell development. Mol Cell Biol 2006;26:789–809.

Published OnlineFirst August 24, 2012; DOI: 10.1158/1078-0432.CCR-12-0861

10. Freedman SJ, Sun ZY, Poy F, Kung AL, Livingston DM, Wagner G, et al. Structural basis for recruitment of CBP/p300 by hypoxia-inducible factor-1 alpha. Proc Natl Acad Sci U S A 2002;99:5367–72.
11. Ruas JL, Berchner-Pfannschmidt U, Malik S, Gradin K, Fandrey J, Roeder RG, et al. Complex regulation of the transactivation function of hypoxia-inducible factor-1 alpha by direct interaction with two distinct domains of the CREB-binding protein/p300. J Biol Chem 2010;285: 2601–9.
12. Kung AL, Zabludoff SD, France DS, Freedman SJ, Tanner EA, Vieira A, et al. Small molecule blockade of transcriptional coactivation of the hypoxia-inducible factor pathway. Cancer Cell 2004;6:33–43.
13. Ryan HE, Lo J, Johnson RS. HIF-1 alpha is required for solid tumor formation and embryonic vascularization. EMBO J 1998;17:3005–15.
14. Li L, Lin X, Staver M, Shoemaker A, Semizarov D, Fesik SW, et al. Evaluating Hypoxia-Inducible Factor-1a as a cancer therapeutic target via inducible RNA interference *in vivo*. Cancer Res 2005;65: 7249–58.
15. Semenza GL. Defining the role of hypoxia-inducible factor 1 in cancer biology and therapeutics. Oncogene 2010;29:625–34.
16. Lee K, Zhang HF, Qian DZ, Rey S, Liu JO, Semenza GL. Acriflavine inhibits HIF-1 dimerization, tumor growth, and vascularization. Proc Natl Acad Sci U S A 2009;106:17910–5.
17. Terzuoli E, Puppo M, Rapisarda A, Uranchimeg B, Cao LA, Burger AM, et al. Aminoflavone, a ligand of the aryl hydrocarbon receptor, inhibits HIF-1 alpha expression in an AhR-independent fashion. Cancer Res 2010;70:6837–48.
18. Schwartz DL, Bankson JA, Lemos R, Lai SY, Thittai AK, He Y, et al. Radiosensitization and stromal imaging response correlates for the HIF-1 inhibitor PX-478 given with or without chemotherapy in pancreatic cancer. Mol Cancer Ther 2010;9:2057–67.
19. Mao SC, Liu Y, Morgan JB, Jekabsons MB, Zhou YD, Nagle DG. Lipophilic 2,5-disubstituted pyrroles from the marine sponge Mycale sp inhibit mitochondrial respiration and HIF-1 activation. J Nat Prod 2009;72:1927–36.
20. Belozerov VE, Van Meir EG. Inhibitors of hypoxia-inducible factor-1 signaling. Curr Opin Investig Drugs 2006;7:1067–76.
21. Tan C, de Noronha RG, Roecker AJ, Pyrzynska B, Khwaja F, Zhang Z, et al. Identification of a novel small-molecule inhibitor of the hypoxia-inducible factor 1 pathway. Cancer Res 2005;65:605–12.
22. Narita T, Yin S, Gelin CF, Moreno CS, Yepes M, Nicolaou KC, et al. Identification of a novel small molecule HIF-1α translation inhibitor. Clin Cancer Res 2009;15:6128–36.
23. Kang SH, Cho HT, Devi S, Zhang Z, Escuin D, Liang Z, et al. Antitumor effect of 2-methoxyestradiol in a rat orthotopic brain tumor model. Cancer Res 2006;66:11991–7.
24. Kaluz S, Kaluzova M, Stanbridge EJ. Does inhibition of degradation of hypoxia-inducible factor (HIF) alpha always lead to activation of HIF? Lessons learnt from the effect of proteasomal inhibition on HIF activity. J Cell Biochem 2008;104:536–44.
25. Nicolaou KC, Pfefferkorn JA, Mitchell HJ, Roecker AJ, Barluenga S, Cao G-Q, et al. Natural product-like combinatorial libraries based on privileged structures. 2. Construction of a 10,000-membered benzopyran library by directed split-and-pool chemistry using NanoKans and optical encoding. J Am Chem Soc 2000;122:9954–67.
26. Tan C, de Noronha RG, Devi NS, Jabbar AA, Kaluz S, Liu Y, et al. Sulfonamides as a new scaffold for hypoxia inducible factor pathway inhibitors. Bioorg Med Chem Lett 2011;21:5528–32.
27. Ishii N, Maier D, Merlo A, Tada M, Sawamura Y, Diserens AC, et al. Frequent co-alterations of TP53, p16/CDKN2A, p14ARF, PTEN tumor suppressor genes in human glioma cell lines. Brain Pathol 1999;9: 469–79.
28. Kaluz S, Kaluzova M, Stanbridge EJ. Expression of the hypoxia marker carbonic anhydrase IX is critically dependent on SP1 activity. Identification of a novel type of hypoxia-responsive enhancer. Cancer Res 2003;63:917–22.
29. Kern SE, Kinzler KW, Bruskin A, Jarosz D, Friedman P, Prives C, et al. Identification of p53 as sequence-specific DNA-binding protein. Science 1991;252:1708–11.
30. Kaur B, Brat DJ, Devi NS, Van Meir EG. Vasculostatin, a proteolytic fragment of brain angiogenesis inhibitor 1, is an antiangiogenic and antitumorigenic factor. Oncogene 2005;24:3632–42.
31. Kaur B, Cork SM, Sandberg EM, Devi NS, Zhang Z, Klenotic PA, et al. Vasculostatin inhibits intracranial glioma growth and negatively regulates *in vivo* angiogenesis through a CD36-dependent mechanism. Cancer Res 2009;69:1212–20.
32. Van Meir EG. Identification of nude mice in tumorigenicity assays. Int J Cancer 1997;71:310.
33. r-xenocat. [cited May 28 2012] Available from: http://code.google.com/p/r-xenocat/.
34. Mooring SR, Jin H, Devi NS, Jabbar AA, Kaluz S, Liu Y, et al. Design and synthesis of novel small-molecule inhibitors of the hypoxia inducible factor pathway. J Med Chem 2011;54:8471–89.
35. Mun J, Jabbar AA, Devi NS, Liu Y, Van Meir EG, Goodman MM. Structure–activity relationship of 2,2-dimethyl-2H-chromene based arylsulfonamide analogs of 3,4-dimethoxy-N-[(2,2-dimethyl-2H-chromen-6-yl)methyl]-N-phenylbenzenesulfonamide, a novel small molecule hypoxia inducible factor-1 (HIF-1) pathway inhibitor and anti-cancer agent. Bioorg Med Chem 2012;20:4590–7.
36. Mun J, Jabbar AA, Devi NS, Yin S, Wang Y, Tan C, et al. Design and *in vitro* activities of N-alkyl-N-[(8-R-2,2-dimethyl-2H-chromen-6-yl) methyl]heteroarylsulfonamides, novel small molecule hypoxia inducible factor-1 (HIF-1) pathway inhibitors and anti-cancer agents. J Med Chem 2012;55:6738–50.
37. Post DE, Van Meir EG. Generation of bidirectional hypoxia/HIF-responsive expression vectors to target gene expression to hypoxic cells. Gene Ther 2001;8:1801–7.
38. Wang W, Ao L, Rayburn ER, Xu H, Zhang X, Xu Z, et al. KCN1, a novel synthetic sulfonamide anticancer agent: *in vitro* and *in vivo* antipancreatic cancer activities and preclinical pharmacology. PLOS One. 7(9): e44883. doi:10.1371/journal.pone.0044883.
39. Bowers VD, Locker S, Ames S, Jennings W, Corry RJ. The hemodynamic effects of Cremophor-EL. Transplantation 1991;51:847–50.
40. Gelderblom H, Verweij J, Nooter K, Sparreboom A. Cremophor EL: the drawbacks and advantages of vehicle selection for drug formulation. Eur J Cancer 2001;37:1590–8.
41. Shi Q, Yin S, Kaluz S, Ni N, Devi NS, Mun J, et al. Binding model for the interaction of anticancer arylsulfonamides with the p300 transcription cofactor. ACS Med Chem Lett 2012;3:620–5.
42. Post DE, Devi NS, Li Z, Brat DJ, Kaur B, Nicholson A, et al. Cancer therapy with a replicating oncolytic adenovirus targeting the hypoxic microenvironment of tumors. Clin Cancer Res 2004;10: 8603–12.
43. Post DE, Van Meir EG. A novel hypoxia-inducible factor (HIF) activated oncolytic adenovirus for cancer therapy. Oncogene 2003;22:2065–72.
44. Post DE, Sandberg EM, Kyle MM, Devi NS, Brat DJ, Xu Z, et al. Targeted cancer gene therapy using a hypoxia inducible factor dependent oncolytic adenovirus armed with interleukin-4. Cancer Res 2007;67:6872–81.
45. Kim H, Peng G, Hicks JM, Weiss HL, Van Meir EG, Brenner MK, et al. Engineering human tumor-specific cytotoxic T cells to function in a hypoxic environment. Mol Ther 2008;16:599–606.
46. Yang L, Cao Z, Li F, Post DE, Van Meir EG, Zhong H, et al. Tumor-specific gene expression using the survivin promoter is further increased by hypoxia. Gene Ther 2004;11:1215–23.
47. Belozerov VE, Van Meir EG. Hypoxia inducible factor-1: a novel target for cancer therapy. Anticancer Drugs 2005;16:901–9.
48. Semenza GL. HIF-1 inhibitors for cancer therapy: from gene expression to drug discovery. Curr Pharm Des 2009;15:3839–43.
49. Kong DH, Park EJ, Stephen AG, Calvani M, Cardellina JH, Monks A, et al. Echinomycin, a small-molecule inhibitor of hypoxia-inducible factor-1 DNA-binding activity. Cancer Res 2005;65:9047–55.
50. Cook KM, Hilton ST, Mecinovic J, Motherwell WB, Figg WD, Schofield CJ. Epidithiodiketopiperazines block the interaction between hypoxia-inducible factor-1α (HIF-1α) and p300 by a zinc ejection mechanism. J Biol Chem 2009;284:26831–8.

Published OnlineFirst August 24, 2012; DOI: 10.1158/1078-0432.CCR-12-0861

Clinical Cancer Research

Arylsulfonamide KCN1 Inhibits *In Vivo* Glioma Growth and Interferes with HIF Signaling by Disrupting HIF-1 α Interaction with Cofactors p300/CBP

Shaoman Yin, Stefan Kaluz, Narra S. Devi, et al.

Clin Cancer Res Published OnlineFirst August 24, 2012.